International Journal of Latest Research in Science and Technology
Volume 3, Issue 3: Page No. 40-46. May-June 2014
https://www.mnkpublication.com/journal/ijlrst/index.php
ISSN (Online):2278-5299

UNDERSAMPLED INFORMATION RECOVERY IN OFDM ENVIRONMENT

Nikos Petrellis
Computer Science and Engineering Dept., Technological Educational Institute of Thessaly, Greece

Abstract*– An under-sampling technique that can be applied in an Orthogonal Frequency Division Multiplexing (OFDM) environment is presented in this paper. It allows the recovery of sparse input data, at the side of the receiver with fewer samples than the ones required by the Nyquist theorem. It is based on the fact that several samples can be replaced by others that have already been obtained at the side of the receiver if the input data are sparse and some properties of the Discrete Fourier Transform (DFT) are exploited. The Forward Error Correction (FEC) techniques employed can also assist in achieving a lower error in the recovery process. The proposed deterministic technique can be implemented with very low complexity hardware in contrast with Compressive Sampling techniques that require complicated optimization problems to be solved. The sampling of up to ¼ of the samples can be avoided at the side of the receiver reducing the size of the buffer memory used by the FFT, as well as the power consumption of the Analog Digital Converter at the receiver since a lower sampling rate is used at specific time intervals.

Keywords – OFDM, Undersampling, DFT, Analog Digital Conversion

I. INTRODUCTION

Although a signal has to be sampled at a rate that is at least twice its higher frequency component according to the Nyquist theorem, sparse signals can be reconstructed with fewer samples as shown in the Compressive Sampling (CS) approaches. The data recovery is performed in these cases using a very small number of samples. If the original data are not sparse, the difference between successive samples may be sparse and CS techniques are often applied to these sample value differences in the same way. An $M \times N$ matrix is considered to be S-sparse if only S of its values are non zero with $S << M \times N$. The sparse level is expressed here as a fraction of the non-trivial values. For example, a signal with S% sparsity means that S% of the signal values are non-zero.

Kalman Filters are a popular technique for an input signal reconstruction [1]. They can be used for tracking the value of dynamic parameters in noisy environments. They can also be used for input data recovery from fewer samples. Kalman filters are based on a two step recursive process, in the first step the current state variables are estimated (prediction) and the second stage updates the estimated values when the next measurement is available. Real time signal reconstruction approaches based on Kalman filters have been implemented in hardware as is the case in [2].

Kalman filters are also employed by some CS techniques [3][4]. The CS techniques are based on optimization problems that are solved by not deterministic processes that are difficult to implement in hardware. One of the first approaches in this field has been published in [5]. A CS technique that can be implemented with lower complexity hardware has been proposed in [6]. A CS problem can be modeled in the following simplified form:

$$y = Ax + e \quad (1)$$

The N_d-size vector x is the input signal, the M-size vector y is the actual measurement (with $M << N_d$) and e is an M-size error or quantization noise vector. Equation (1) has multiple solutions and a CS method finds an appropriate vector x that fits equation (1) with an acceptable approximation error e. The optimization target that has been proposed in various CS approaches for finding such an appropriate solution for vector x is:

$$\min \|Ax\|_1 \quad (2)$$

Subject to

$$\|y - Ax\|_p \le T \quad (3)$$

The difference between y and $A \cdot x$ (expressed as an L_p norm) is restricted below a threshold T. The matrix A can be expressed as a product of other matrices with special features (e.g., partial Fourier or Hamadad matrices) while the optimization target of (2) can be applied to the product of these matrices with x. Such optimization problems can be solved by iterative or greedy algorithms (basis pursuit, gradient project, gradient pursuit, etc). All of these methods can be easily implemented in software but require high complexity hardware canceling the benefit from the use of a low cost ADC with lower speed and power consumption.

Surveillance and other image processing applications have also adopted CS techniques [7-9]. CS techniques have also been used in OFDM environments for the channel estimation [10]. However, they have not been used for the recovery of the original data and this is not a surprise since the inherent data sparseness is cancelled in an OFDM environment by the FEC encoding, the interleaving and the (I)DFT processes.

The proposed undersampling approach is not based on iterative, recursive or non-deterministic optimization problems. The only operations required are an appropriate interleaving scheme and a simple sparse data detector module at the side of the receiver that a) deactivates specific butterfly sub-blocks of the Fast Fourier Transform (FFT) module, b) controls the sampling rate of the Analog Digital Converter

Publication History
Manuscript Received : *25 June 2014*
Manuscript Accepted : *28 June 2014*
Revision Received : *29 June 2014*
Manuscript Published : *30 June 2014*

(ADC) and c) substitutes the samples that have not been obtained with other available ones at the FFT input. There are also some restrictions concerning the data rate of the employed FEC method.

A higher number of samples are required by the proposed technique (compared to the CS ones) but this is compensated by the very low cost and complexity hardware required. The proposed system has been modeled in MATLAB. All the combinations between 16-QAM or 32-QAM (Quadrature Amplitude Modulation) and 1024 or 4096 point FFT have been tested. Four and 16 pilots have used for the case of 1024 and 4096-point FFT respectively. The results from the simulation of these models show that the Bit Error Rate (BER) is zero or below 10^{-4} using the proposed method if the channel Signal to Noise Ratio (SNR) and the sparse level is good enough.

The principle of operation of the proposed undersampling method has been described by the author in [11] and [12] for 1024-point FFT, 16-QAM modulation and 4 pilots. The use of the proposed method with a variety of QAM modulation schemes and FFT package sizes described in this paper proves that several communication standards could benefit from the proposed undersampling scheme. Moreover, details about the FFT implementation and the architecture of the whole system are given in this paper.

The architecture of an OFDM system and the modifications needed to support the proposed undersamping method is described in Section II. The theory behind the proposed technique is discussed in Section III. Finally, simulation results are presented in Section IV.

II. THE OFDM ARCHITECTURE

Figure (1) shows the architecture of an OFDM system with the necessary additional modules to support the proposed method. At the side of the transmitter the input data bit stream is encoded by the employed FEC encoder that generates the parity bits that will be used at the receiver to correct potential errors that would occur during the transmission (e.g., due to channel noise). The FEC encoder is characterized by its data rate R that represents the fraction between the data and the total bits at its output. For example, if R=1/2, then half of the bits at the FEC encoder output are data and the rest are parity bits.

The data and parity bits are interleaved and then mapped to constellations according to the employed QAM scheme. A number of pilots with constant values are placed among the resulting QAM symbols in order to equalize the channel subcarriers at the receiver. The resulting packet can be padded with guard symbols to form the input to an Inverse-Discrete Fourier Transform (IDFT) consisting of N complex inputs X_k. The IDFT is implemented as an Inverse Fast Fourier Transform (IFFT). A Cyclic Prefix (CP) is usually added at the front of the packet of the N complex IDFT outputs x_n to avoid inter-symbol interference. The transmission can be carried out either at the baseband or over a higher frequency carrier. The high frequency carrier modulation/ demodulation stages have not been described in Fig. 1 since they do not affect the proposed method. A Additive White Gaussian Noise (AWGN) channel is also assumed as is the case in wired communications.

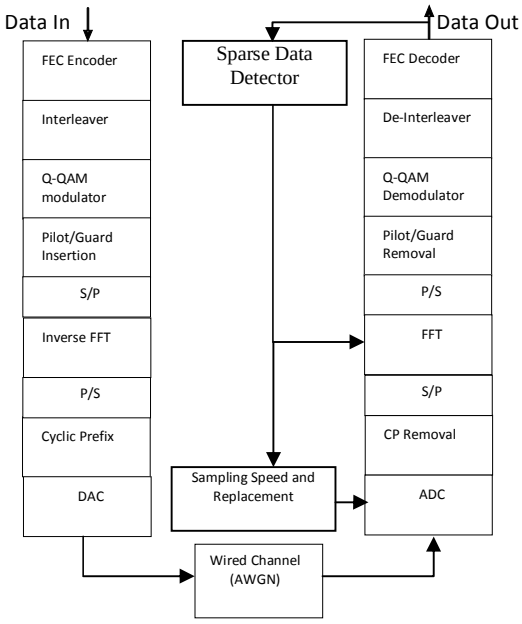

Fig. 1 The Architecture of an OFDM system

At the side of the receiver, an ADC samples the received signal in order to obtain the x_n symbols. The CP symbols are ignored while the rest of the x_n symbols include the payload, the pilots and the padding symbols. The sample values acquired by the ADC that form the FFT input as well as the output of the FFT (X_k) have to be buffered by the Serial to Parallel (S/P) and the Parallel to Serial (P/S) modules. The padding symbols as well as the pilots are removed from the FFT output and the rest of the X_k QAM symbols are mapped to the bits they correspond to. The resulting bit stream is De-interleaved and feeds a FEC decoder that corrects any errors that can be recognized.

According to the proposed undersampling scheme, each one of the Q-QAM symbols generated at the transmitter can be derived either from data or parity bits and not from both of them. Thus, the interleaver is allowed to permute data bits or parity bits within a single group of log_2Q bits or permute Q-QAM symbols provided that Q-QAM data symbols will remain at the odd positions as will be described in the next section. The data rate of the FEC encoder should also be higher than ½ in order to have enough data Q-QAM symbols at all the odd positions of the IFFT input.

Of course, at the side of the receiver the employed De-interleaving and FEC decoding schemes must comply with the ones adopted at the transmitter. The data bit stream at the output of the FEC decoder is observed in order to detect sparse data transmission. In most cases sparse data exchange will last for a large number of successive N-point FFT transforms. The Sparse Data Detector (see Fig. 1) at the side of the receiver may count the number of successive trivial bits (e.g., with value 0) and if large sequences of sparse data are detected the receiver may enter the "Undersampling Mode". When the Sparse Data Detector finds that the output data are not sparse anymore, it will exit the "Undersampling Mode". It is possible that the output data will have a large error during the time interval between the ending of the

sparseness and the "Undersampling Mode" deactivation, but this can be tuned to be short enough by the Sparse Data Detector according to the type of applications that use the proposed telecommunication system architecture.

In the "Undersampling Mode", the Sampling Speed and Replacement module (see Fig. 1) samples the receiver input signal at half speed for up to 25% of the time as will be described in the next section. The samples that will be omitted in these undersampling intervals (up to 25%) are replaced by other samples already retrieved.

In the "Undersampling Mode" up to half of the FFT circuitry can also be deactivated (i.e., one of the two *N/2*-point FFT butterflies). As will be shown in Section IV, if the undersampling is applied to 25% of the samples/time and correspondingly half of the FFT circuitry is turned off, an high error floor occurs. However, operating in "Undersampling Mode" in 12.5% of the time is a more realistic scenario. In this case, the ADC would dissipate half power since the power consumption is proportional to the operating frequency. Moreover, a quarter of the FFT circuitry (a *N/4*-point FFT butterfly) could be turned off and the buffering memory as well as the speed can also be improved by the same amount as will be discussed in the following sections.

III. THE CONCEPT OF THE PROPOSED UNDERSAMPLING METHOD

The DFT and IDFT operations are defined by the equations (4) and (5) respectively:

$$X_k = \sum_{n=0}^{N-1} x_n w_N^{kn} \text{ ,, } 0 \le k < N-1 \quad (4)$$

$$x_n = \sum_{k=0}^{N-1} X_k W_N^{kn} \text{ ,} 0 \le n < N-1 \quad (5)$$

The twiddle factors W_N^{kn} and w_N^{kn} are defined as:

$$W_N^{kn} = e^{j\frac{2\pi kn}{N}} \quad (6)$$

$$w_N^{kn} = e^{-j\frac{2\pi kn}{N}} \quad (7)$$

and $j^2=-1$. It can be proven that the symbols x_{2p+1} with p between 0 and *N/4-1* are equal to the symbols $x_{2p+1+N/2}$, provided that $X_{2t+1}=X_{2t+1+N/2}$, for t between 0 and *N/4-1*. Equation (5) can be rewritten for x_{2p+1} as:

$$x_{2p+1} = \sum_{k=0}^{N-1} X_k e^{j2\pi k(2p+1)/N} = \sum_{k=0}^{N-1} X_k e^{j4\pi kp/N} e^{j2\pi k/N} \quad (8)$$

while $x_{2p+1+N/2}$ can be estimated as:

$$x_{2p+1+N/2} = \sum_{k=0}^{N-1} X_k e^{j2\pi k(2p+1+N/2)/N} = \sum_{k=0}^{N-1} X_k e^{j4\pi kt/N} e^{j2\pi k/N} e^{j\pi k} = \sum_{k=0}^{N-1} X_k e^{j4\pi kt/N} e^{j2\pi k/N} (-1)^k \quad (9)$$

As can be seed from equations (8) and (9), $x_{2p+1} = x_{2p+1+N/2}$ only if the X_k at the odd positions are 0. This is not a very useful property for the case of the QAM modulation since there are no QAM symbols with 0 value. Nevertheless, if the terms in the summations of equations (8) and (9) are grouped in pairs that include X_k symbols with distance *N/2*, then for a single pair with odd k we would have:

$$X_k e^{j2\pi k(2t+1)/N} + X_{k+N/2} e^{j2\pi (k+N/2)(2t+1)/N} = X_k e^{j4\pi kt/N} e^{j2\pi k/N} - X_{k+N/2} e^{j4\pi kt/N} e^{j2\pi k/N} \quad (10)$$

As can be shown from equation (9) it is sufficient to have $X_k=X_{k+N/2}$ when k is odd ($k=2t+1$). This can be achieved if the QAM symbols are derived by sparse data (e.g., 0) since in this case almost all of the X_{2t+1} symbols will have the same value (QAM equivalent of 0). If $X_k=X_{k+N/2}$ holds for almost all odd $k<N/2$, then all the X_k symbols with odd k add up to a zero or near zero value. This can be achieved if the X_k symbols with odd k are derived by sparse data. In this case, half of the x_n symbols at the odd positions can substitute the rest of the x_n symbols with odd n. The number of the substituted samples can be further increased if the X_k values are correlated with specific rules.

The sparse data X_k symbols can be placed at odd k-positions, by an appropriate interleaving and FEC encoding scheme. A few X_k symbols will not be equal to the trivial common value X_c, since the input data have a high sparseness level but they are not all zero. As already mentioned the data rate R of the employed FEC encoder, should be greater or equal than 1/2. If $R=1/2$, the data and the parity bits can be grouped separately by the Q-QAM modulator of Fig. 1 and half of the Q-QAM symbols will correspond to data having the same trivial value X_c. The symbols with X_c value should be placed by the interleaver at the odd positions. The proposed method is still applicable if R>1/2 since additional data symbols with X_c value will be placed at even positions. It is not recommended however to use FEC encoders with $R<1/2$ because some parity symbols will have to be placed at odd positions and these parity symbols will probably not have an X_c value.

Optimal interleaving strategies depend on many factors like, the data rate R, the decoding algorithm used, its randomness, the minimum distance where a value should be moved, etc. For example, the higher the data rate R is, the

higher is the BER [13]. Moreover, a difference in the BER in the order of 10^{-3} can be observed between different interleaving schemes for the same SNR[13]. As can be deduced by the analysis on equation (10), the interleaver in the proposed method is allowed to do any permutation separately in the data and the parity bit stream. It is also allowed to permute in a random way the data *Q*-QAM symbols between odd positions and the parity *Q*-QAM symbols between even positions (channel interleaving) but it is not allowed to move data symbols to even positions and parity symbols to odd positions.

The position of pilots and the padding symbols has also to be taken into account by the interleaver. A value equal to X_c is also selected for these symbols. In this work, the FEC encoder is implemented as a Recursive Convolutional Systematic (RSC) encoder with a systematic and a parity output with data rate *R=1/2*. The feedforward path is described by the polynomial $1+D+D^2+D^3$ and the feedback path is described by $1+D+D^2$. A Viterbi decoder is used at the side of the receiver. A small $2\times log_2Q$-bit buffer is used at the output of the encoder to group the log_2Q data and log_2Q parity bits into a pair of *Q*-QAM symbols.

The structure of the IFFT input packets for the case of a 1024 and a 4096-point FFT are shown in Fig. 2, in order to demonstrate how the interleaver should place the data, parity, pilot and padding symbols. In both cases it is assumed that 25% of the packet is padding. In the example of the 1024-point FFT (Fig. 2a), 4 pilots are used. After 96 padding symbols the 1st pilot appears (Pt1 at the position No. 96). The data (D) and parity (P) *Q*-QAM symbols follow. A data symbol should be placed first since the position No. 97 is odd. Then the rest of the symbols are placed in an alternating manner (DPDP.. or PDPD..) in order to reassure that data symbols are placed in the odd positions. The second pilot (Pt2) appears at an odd position, thus the following sequence must start with a parity symbol in order to reassure that data symbols continue to be placed at odd position. In the same way the sequence for the rest of the data and parity symbols is determined as shown in Fig. 2a. In this example the parity and data sequences form segments of 192 symbols separated by pilots.

In the same way the 4096 symbol packet is constructed at Fig. 2b. In this case, 16 pilots are used, but the 16 parity/data segments still consist of 192 symbols. In both cases, the specific *Q*-QAM modulation used does not affect the structure although the total number of bits differs according to the *Q* value used. For example, in the case of 1024-point FFT and 16-QAM, 1536-bits are transferred within each packet while 1920-bits are transferred within the same packet structure if 32-QAM is used.

Some blocks of the FFT module used at the receiver can also be deactivated when specific FFT inputs have the same value as can be seen from Fig. 3 where the butterflies of an *N*-point FFT are shown. The even positioned x_n values are inputs to an *N/2* FFT. The odd positioned x_n values form pairs of equal values: (x_{2p+1}, $x_{2p+1+N/2}$) that are inputs to 2-point FFTs. The outputs of the 2-point FFTs and consequently the ones of the higher radix FFTs that are constructed using these 2-point FFTs are all zero since:

$$\sum_{n=0}^{N-1} w_N^{kn} = 0 \qquad (11)$$

The bottom *N*/2-point FFT of Fig. 3, does not contribute to the estimation of all the outputs of the *N*-bit FFT and can be deactivated or omitted if the data exchanged over the OFDM environment are permanently sparse. The implementation of the FFT would require only half of the die area in this case. If sparse data are only occasionally exchanged and detected by the Sparse Data Detector of Fig. 1, a die area reduction is inevitable but at least the FFT power consumption can be significantly reduced when some butterflies are turned off.

IV. SIMULATION RESULTS

The system described in Fig. 1 was modeled in MATLAB and configured to simulate the FFT symbol packets of Fig. 2 for 16 and 32 QAM as shown in Fig. 4-6. The specific combinations tested were: a) 16-QAM, 1024-point FFT (Fig. 4), b) 32-QAM, 1024-point FFT (Fig. 5), c) 16-QAM, 4096-point FFT (Fig. 6) and d) 32-QAM, 4096-point FFT. In each one of these cases pseudorandom inputs with three levels of sparseness were used: 0.5%, 1% and 2%. Finally, all of these cases were tested for 25%, 12.5%, 6.25%, 3.125% sample replacement. The option where no samples are replaced was also considered as a reference in each case.

One of the conclusions that can be drawn by observing Fig. 4-7 is that 32-QAM performs worse than 16-QAM. Generally speaking, the probability of having a non-zero bit within the log_2Q bits of a QAM symbol is higher as *Q* increases. In this way, a larger number of QAM symbols has a value different from V_c. Thus, the proposed undersampling method is more efficient for *Q*-QAM modulations with lower *Q*. The size of the FFT input symbol packet is not important at least when the padding level is similar.

Although the error floor for 25% sample replacement is too high, the error floor of 12.5% sample replacement can be acceptable (close to 10^{-3} or lower) if the sparseness level is below 0.5%. If a smaller number of samples is replaced (as in the case of 6.25% or 3.125%) then full input recovery is possible in most of the sparseness levels tested, if the channel SNR is high enough.

Although a direct comparison with the referenced approaches is not possible since different metrics are used according to the target applications of each method, the basic features of three of the referenced approaches are listed in Table 1. In [7] the Normalized Mean Square Error (NMSE) is used to measure the efficiency of the proposed method. the number of samples used to reconstruct an image of 650 pixels ranges from 120 to 320. The corresponding NMSE in our approach is much lower than 0.1 in many cases. The case study of the reaction 1H-1H COSY spectrum is used from reference [8]. In [10] the OFDM channel response is estimated using a small number of pilots as shown in the second column of Table 1. The achieved BER is shown in the third column for specific channel SNR conditions.

Padding (96 symbols)	Pt1	DPDPDPD…DP (192 symbols)	Pt2	PDPDPDP…PD (192 symbols)	Pt3	DPDPDPD…DP (192 symbols)	Pt4	PDPDPDP…PD (192 symbols)	Padding (156 symbols)

(a)

Padding (384 symbols)	Pt1	DPDPDPD…DP (192 symbols)	Pt2	PDPDPDP…PD (192 symbols)	…	Pt 16	PDPDPDP…PD (192 symbols)	Padding (624 symbols)

(b)

Fig. 2 FFT packet structure tested for 1024-points (a) and 4096-points (b)

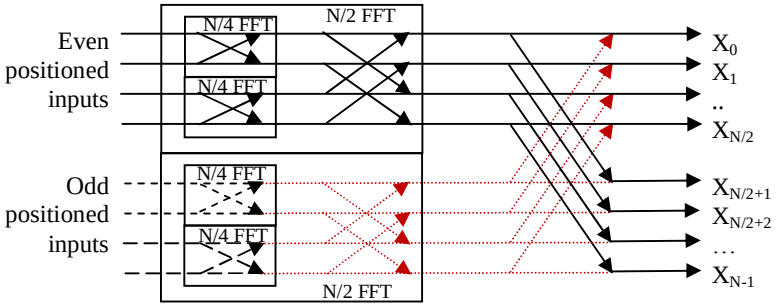

Fig. 3 Deactivated FFT butterflies (with red color outputs) when the odd positioned inputs have the same value

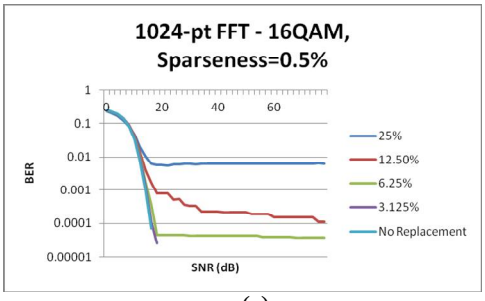

(a)

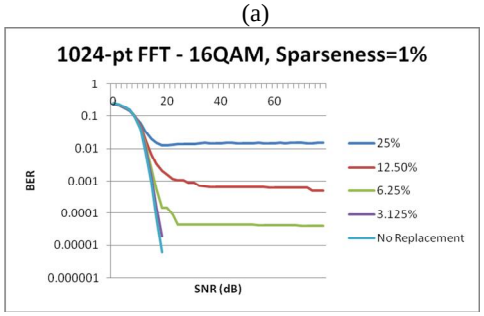

(b)

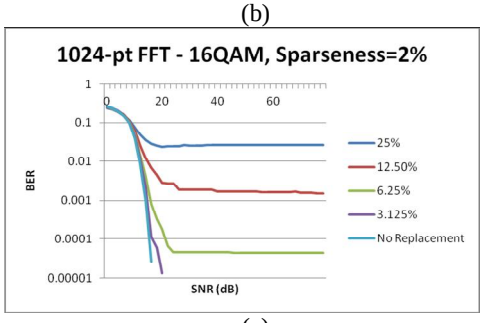

(c)

Fig. 4 1024-point FFT with 16-QAM for 0.5% (a), 1% (b) and 2% (c) sparseness and for 5 sample replacement cases (25%, 12.5%, 6.25%, 3.125% and 0%)

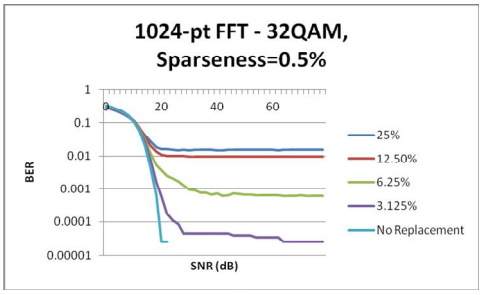

(a)

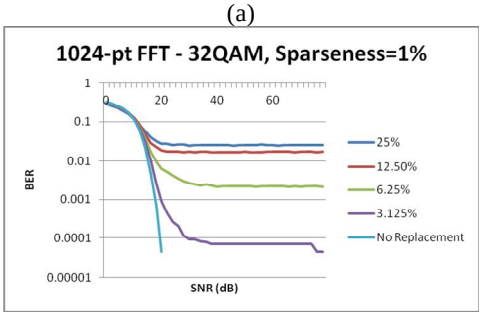

(b)

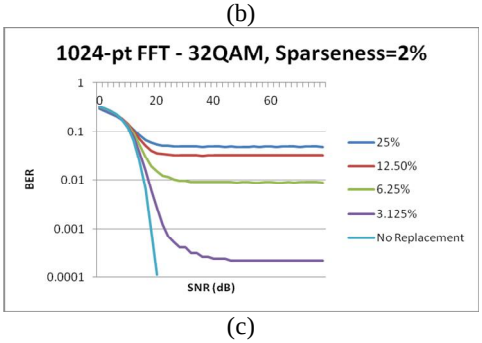

(c)

Fig. 5 1024-point FFT with 32-QAM for 0.5% (a), 1% (b) and 2% (c) sparseness and for 5 sample replacement cases (25%, 12.5%, 6.25%, 3.125% and 0%)

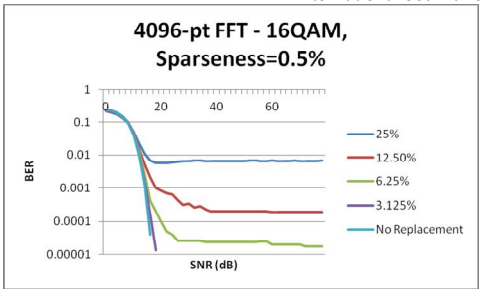

(a)

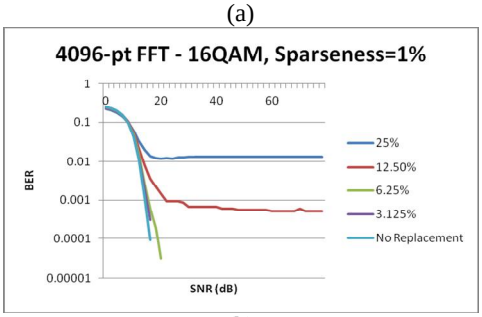

(b)

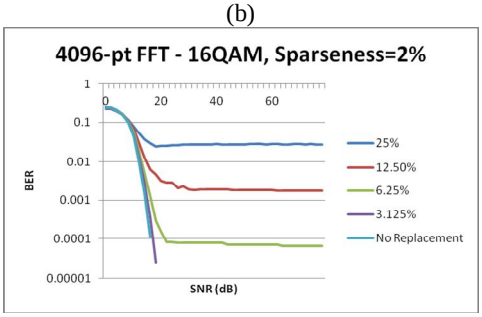

(c)

Fig. 6 4096-point FFT with 16-QAM for 0.5% (a), 1% (b) and 2% (c) sparseness and for 5 sample replacement cases (25%, 12.5%, 6.25%, 3.125% and 0%)

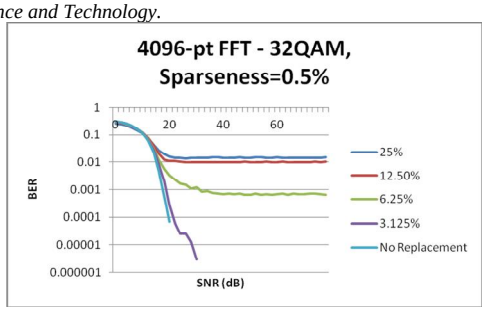

(a)

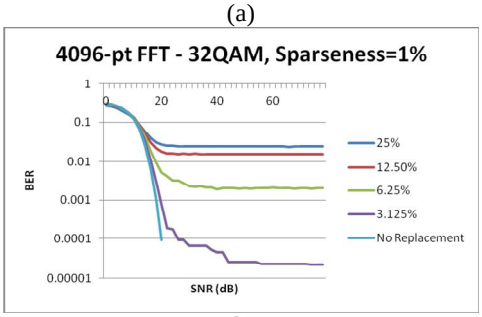

(b)

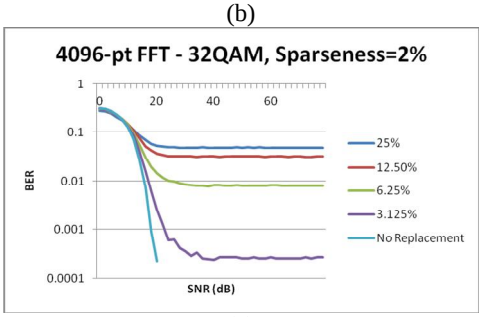

(c)

Fig. 7 4096-point FFT with 32-QAM for 0.5% (a), 1% (b) and 2% (c) sparseness and for 5 sample replacement cases (25%, 12.5%, 6.25%, 3.125% and 0%)

TABLE I COMPARISON WITH REFERENCED APPROACHES

Reference	**Used Samples**	**Error**
This work	896 of 1024 (0.5% sparsity, 16-QAM)	BER≈10^{-4} @ SNR=40dB
[7]	120-320 from 650	NMSE ≈ 0.18
[8]	0.20 sampling rate fraction	Error: 0.007
[10]	224 pilots in 1024 subcarriers	BER=10^{-4} @ SNR=12dB

V. CONCLUSIONS

An undersampling method that can be implemented with low complexity hardware in an OFDM environment was presented in this paper. It was tested using different size FFTs and QAM modulation methods. Up to ¼ of the samples at the receiver can be substituted by other available samples, reducing the power consumption of the ADC and the FFT as well as the size of the memory needed to store the ADC samples. The input data recovery can be achieved with zero or very low error.

Future work will focus on the investigation of the efficiency of the proposed undersampling method in wireless and Multiple In, Multiple Out (MIMO) channels. Moreover, FEC methods other than Viterbi will be studied like LDPC and Turbo Codes.

ACKNOWLEDGMENT

This work is protected under the provisional patent 1008130/6-3-2014 and the provisional patent with Application No. 20140100069 (Greek Patent Office - OBI).

REFERENCES

[1] Carmi, A., Gurfil, P., Kanevsky, D., "Methods for Sparse Signal Recovery Using Kalman Filtering With Embedded Pseudo-Measurement Norms and Quasi-Norms," IEEE Transactions on Signal Processing vol. 58(4), pp. 2405-2409, 2010.

[2] Massicotte, D., "A parallel VLSI architecture of Kalman-filter-based algorithms for signal reconstruction," Elsevier Integration, The VLSI Journal, vol. 28(2), pp. 185-196, 1999.

[3] Vaswani, N., "Kalman filtered compressed sensing," Proceedings of the IEEE Int. Conf. Image Processing (ICIP), pp. 893–896, San Diego (CA), 12-15 Oct 2008.

[4] Kanevsky, D., Carmi, A., Horesh, L., Gurfil, P., Ramabhadran, B., Sainath, T. N., "Kalman Filtering for Compressed Sensing," Proceedings of the 13th Conference on Information Fusion (FUSION), Edimburgh, 26-29 July 2010.

[5] Candès, E.J., Wakin, M.B., "An Introduction To Compressive Sampling," IEEE Signal Processing Magazine vol. 25(2), pp. 25-30, 2008.

[6] Mishali, M., Eldar, Y., "From Theory to Practice: Sub-Nyquist Sampling of the Sparse Wideband Analog Signals," IEEE Journal of Selected Topics in Signal Processing, vol. 4(2), pp. 375-391, 2010.

[7] Mahalanomis, A., and Muise, R., "Object Specific Image Reconstruction using a Compressive Sensing Architecture for Application in Surveillance Systems," IEEE Trans. On Aerospace and Electronic Systems, vol. 45(3), pp. 1167-1180, 2009.

[8] Qu, X., Guo, D., Cao, X., Cai, S., and Chen, Z. "Reconstruction of Self-Sparse 2D NMR Spectra from Undersampled Data in the Indirect Dimension," MDPI Sensors, vol.11, pp. 8888-8909, 2011.

[9] Hardie, R.C., and Droege, D.R., "A MAP Estimator for Simultaneous Superresolution and Detector Nonunifomity Correction," EURASIP Journal on Advances in Signal Processing Article ID 89354, Hindawi Publishing Corp., pp. 1-11, 2007.

[10] Schniter, P., "A Message-Passing Receiver for BICM-OFDM Over Unknown Clustered-Space Channels," IEEE Journal of Selected Topics in Signal Processing, vol. 5(8), pp. 1462-1474, 2011.

[11] Petrellis, N., "Deterministic Under-sampling with Error Correction in OFDM Systems," Proceedings of 17th PCI Conference (ACM), pp. 47-54, Sep. 19-21, 2013 Thessaloniki, Greece.

[12] Petrellis, N., "Information Recovery Using Undersampling in Orthogonal Frequency Division Multiplexing Systems," Proceedings of IEEE DSP 2013, July 1-3, 2013, Santorini, Greece.

[13] Yu, J., Boucheret, M.L., Vallet, R., Duverdier, A., Mesnager, G., "Interleaver Design for Turbo Codes From Convergence Analysis," IEEE Transactions On Communications, vol. 54(4), pp. 619-624, 2006.